ELSEVIER

Spectral properties and statistics of resistive drift-wave turbulence

Dieter Biskamp, Suzana J. Camargo, Bruce D. Scott

Max-Planck-Institut für Plasmaphysik, 85748 Garching bei München, Germany

Abstract

Resistive drift-wave turbulence is studied by high-resolution numerical simulation in the limit of small viscosity (high Reynolds numbers), such that the adiabaticity parameter $\mathscr{C}$ is the only relevant parameter. Energy spectra exhibit a maximum at some wave-number k_0 and a power law behavior for $k > k_0$. Statistics in this range are non-Gaussian indicating strong intermittency, but are perfectly Gaussian for $k \lesssim k_0$.

Drift-wave turbulence is generally believed to cause anomalous transport in magnetically confined plasmas such as those in tokamaks and stellarators. Density and potential fluctuations are particularly strong in the cool plasma edge region, where collisional effects are most important to drift-waves. A simple two-dimensional model to describe drift-wave turbulence in this regime is due to Hasegawa and Wakatani [1,2]. It consists of two equations for the potential and density fluctuations $\varphi(x, y)$, $n(x, y)$ in a plasma with a constant mean density gradient dn_0/dx in the x direction and a magnetic field essentially in the z direction,

$$\partial_t \omega + v \cdot \nabla \omega = \mathscr{C}(\varphi - n) + \mathscr{D}^\omega , \tag{1}$$

$$\partial_t n + v \cdot \nabla n + \partial_y \varphi = \mathscr{C}(\varphi - n) + \mathscr{D}^n , \tag{2}$$

$$v = \hat{z} \times \nabla \varphi ,$$

$$\omega = \nabla^2 \varphi ,$$

written in the usual dimensionless form: $x, y \rightarrow x/\rho_s, y/\rho_s, t \rightarrow (t\Omega_i)(\rho_s/L_n), \varphi \rightarrow (e\varphi/T_e)L_n/\rho_s, n \rightarrow (n/n_0)(L_n/\rho_s), L_n = n_0/|dn_0/dx|; \rho_s$ and Ω_i are the ion Larmor radius and frequency, respectively. $\mathscr{C}$ is

called the adiabaticity parameter due to the electron parallel friction, i.e. resistivity η, $\mathscr{C} = (T_e/n_0 e\eta)k_z^2$, and $\mathscr{D}^\omega$, $\mathscr{D}^n$ are the viscous and diffusive dissipation terms to be specified below. Apart from its potential application to anomalous plasma transport, the Hasegawa–Wakatani model is also interesting in its own right as an autonomous (i.e. self-exciting) system of 2-D turbulence. For $\mathscr{C} \ll 1$ Eq. (1) decouples to the 2-D Navier–Stokes equation, while n is essentially a passive scalar. In the opposite limit $\mathscr{C} \gg 1$, the electrons are almost adiabatic $n - \varphi \ll n$, and Eqs. (1) and (2) are essentially equivalent to the Hasegawa–Mima equation [3]. For the Hasegawa–Wakatani model, the energy $E = \frac{1}{2} \int d^2x (v^2 + n^2)$ and the generalized enstrophy $W = \frac{1}{2} \int d^2x (n - \omega)^2$, which are the invariants of the Hasegawa–Mima equation, follow the equations

$$\frac{dE}{dt} = - \int d^2x \, n \partial_y \varphi - \mathscr{C} \int d^2x \, (\varphi - n)^2$$

$$- \int d^2x \, (\varphi \mathscr{D}^\omega - n \mathscr{D}^n) , \tag{3}$$

$$\frac{dW}{dt} = -\int d^2x \, n\partial_y\varphi + \int d^2x \, (\omega - n)(\mathcal{D}^\omega - \mathcal{D}^n) . \tag{4}$$

The linear stability properties can be easily derived (see e.g. Ref. [3]). It can then be shown that neglecting dissipation all modes are linearly unstable, whereas with finite dissipation terms $\mathcal{D}^\omega$, $\mathcal{D}^n$, high-k and small-k modes are damped. Eqs. (1), (2) have recently been studied by numerical simulation with the emphasis on statistical equilibrium ensembles [4] and coherent structures [5] (the latter well-known from 2-D Navier–Stokes turbulence [7,8]). In contrast to Ref. [5], where the dissipation terms have a strong influence on the turbulence, we are interested in what we call the non-viscous limit: that of small $\mathcal{D}^\omega$, $\mathcal{D}^n$, such that their contribution to the energy dissipation in Eq. (3) is negligible. As has been shown by the statistical equilibria [6] and confirmed via numerical simulation [4], if dissipation is entirely absent then the enstrophy spectrum rises according to $W_k \propto k$ so that it is unbounded. This situation is avoided in this paper by retaining finite $\mathcal{D}^\omega$, $\mathcal{D}^n$ and arranging their effect to be confined to the smallest scales by choosing high-order dissipation operators,

$$\mathcal{D}^\omega = \nu_\omega \Delta^3 \omega, \quad \mathcal{D}^n = \nu_n \Delta^3 n, \quad \nu_\omega = \nu_n = \nu . \tag{5}$$

In the non-viscous limit $\mathscr{E}$ is the only relevant parameter and the sole effect of ν is to determine the extent of the inertial range.

Our numerical simulations are performed on a square box of size $2\pi L \times 2\pi L$ with periodic boundary conditions using a pseudo-spectral method with grid-size varying from 256^2 to 1024^2 grid-points. The algorithm is similar to the one described in Ref. [9]. The numerical simulations are performed for 10^2–10^3 time units after a stationary turbulence is achieved, in order to allow good statistical averages. Three values of $\mathscr{E}$ are considered, $\mathscr{E} = 0.1, 1, 5$; respectively corresponding to the hydrodynamic, intermediate and adiabatic limits. The box size parameter is chosen $L = 6.7$ and $L = 26.7$ to concentrate on primarily high-k and small-k behavior, respectively. The dissipation parameter ν varies from 1×10^{-4}, for $L = 26.7$ and 256^2 grid-points, to 5×10^{-10}, for $L = 6.7$ and 1024^2 grid-points. The aim of this work is the analysis of the spectral properties of the turbulence, their relation to the linear instability properties and the statistics of the turbulence.

The angle integrated energy spectrum E_k, $E = \int dk \, E_k$, shows a maximum at some wave-number $k = k_0$. For $\mathscr{E} \ll 1$ one has $k_0 \simeq k_m$, where $\mathbf{k} = (0, k_m)$ is the most unstable linear mode, while for $\mathscr{E} > 1$, where k_m becomes constant, $k_m \simeq 1.3$, k_0 decreases with increasing $\mathscr{E}$ owing to the inverse energy cascade well-known for the Hasegawa–Mima equation, e.g. $k_0 = 0.4$ for $\mathscr{E} = 5$. While for $k < k_0$ the spectral distribution is anisotropic reflecting the properties for the linear growth rate, it is isotropic for $k > k_0$. In the inertial range, $k_0 < k < k_\nu$, where k_ν indicates the viscous cutoff, E_k exhibits a clear power law (Fig. 1a). The energy spectrum E_k is composed of E_k^V, the kinetic energy spectrum and E_k^N, the density spectrum. Let us first analyse the kinetic energy spectrum (Fig. 1b). Since the effect of the collisional term is small in the inertial range (also for $\mathscr{E} > 1$ where n_k is approximately adiabatic, $n_k \simeq \varphi_k$), Eq. (1) essentially reduces to the 2-D Navier–Stokes equation, where the spectrum $E_k^V \sim k^{-3}(\ln kL)^{-1/3}$ is predicted [10]. We find $E_k^V \sim k^{-\alpha}$, $\alpha = 3.1$–3.5, rather independently of $\mathscr{E}$, which is only slightly steeper than the effective theoretical value $\alpha_{\text{eff}} \simeq 3.1$ and closer to the latter than observed in simulations of 2-D Navier–Stokes turbulence [8,11]. On the other hand, the density spectrum depends on $\mathscr{E}$. For $\mathscr{E} \ll 1$, where the density behaves essentially as a passively advected scalar, analogy with the 2-D Euler equation for the vorticity suggests a spectrum $E_k^N \sim k^2 E_k^V$, which is in fact observed, $E_k^N \sim k^{-1.6}$ for $\mathscr{E} = 0.1$. Since $E^N \gg E^V$, the energy spectrum is primarily given by the density spectrum, $E_k \simeq E_k^N$. In the opposite case $\mathscr{E} \gg 1$, where $n_k \simeq \varphi_k$, the density contribution to the energy spectrum is small, $E_k \simeq E_k^V \gg E_k^N$.

Let us compare the nonlinear turbulent behavior with the quasilinear prediction, considering in particular the turbulent flux Γ,

$$\Gamma = \langle v_x n \rangle = i \int d^2k \, k_y n_k \varphi_k^* . \tag{6}$$

It has previously been noted [5] that $\Gamma \simeq \Gamma_{\text{ql}}$, the quasilinear expression, for $\mathscr{E} > 1$, while $\Gamma < \Gamma_{\text{ql}}$ for $\mathscr{E} < 1$, $\Gamma/\Gamma_{\text{ql}}$ decreasing with decreasing $\mathscr{E}$. In the non-viscous limit we find approximately $\Gamma/\Gamma_{\text{ql}} \sim \mathscr{E}^{1/3}$ for $\mathscr{E} < 1$. Considering the spectral properties Γ_k of the
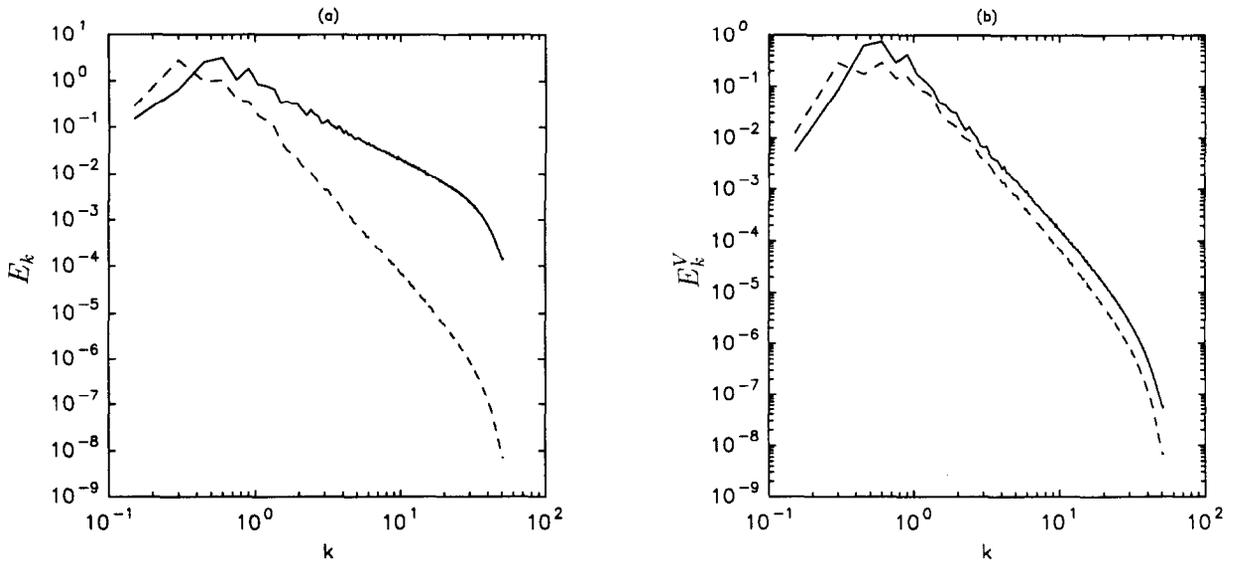
Fig. 1. (a) Energy spectrum for $\mathscr{C}=0.1$ (full line) and $\mathscr{C}=5$ (dashed line). (b) Kinetic energy spectrum for the cases as in (a).

flux, $\Gamma = \int dk\,\Gamma_k$, we observe that Γ_k agrees precisely with $(\Gamma_{ql})_k$ for $k < k_0$, while the latter exceeds the former for $k > k_0$ by about a constant value increasing with decreasing $\mathscr{C}$ (Fig. 2). For $\mathscr{C}=5$ we have $\Gamma_k = (\Gamma_{ql})_k$ over the entire spectrum. This agreement may be somewhat surprising, since for $\mathscr{C} \gg 1$ the energy spectrum is more strongly influenced by the

nonlinear inverse cascade process than by the linear stability properties. However, in this range nonlinear fluctuations behave essentially as linear drift-waves, such that weak turbulence theory is approximately valid.

The statistical properties are conveniently described by the normalized structure functions, in par-
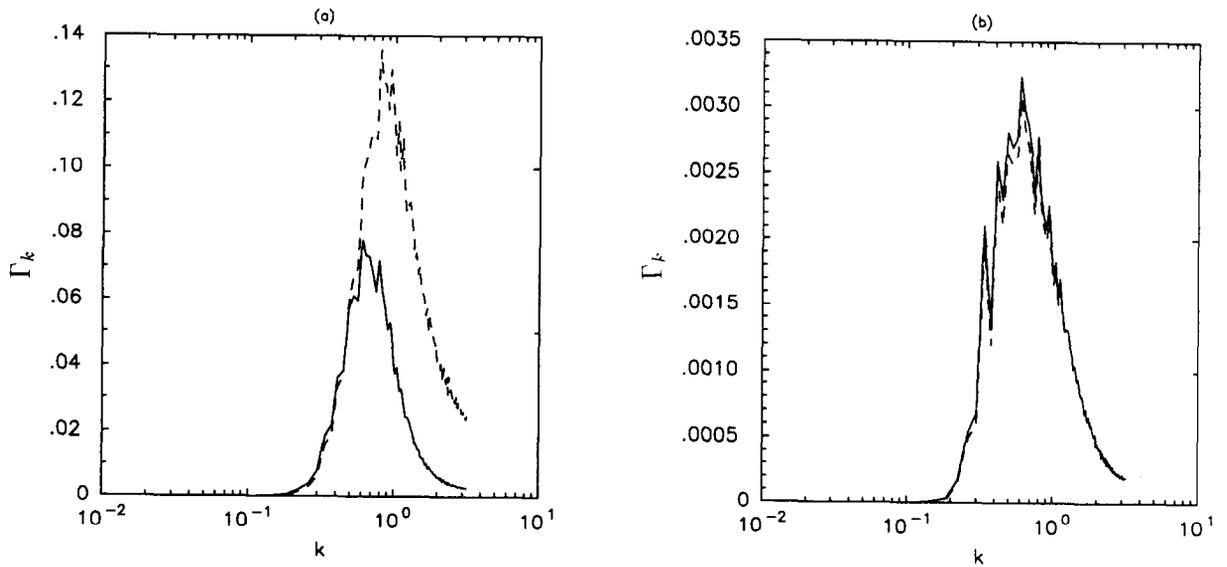
Fig. 2. Spectral distributions of the nonlinear (full lines) and quasi-linear (dashed lines) fluxes, Γ_k and $(\Gamma_{ql})_k$ respectively. (a) $\mathscr{C}=0.1$; (b) $\mathscr{C}=5$.
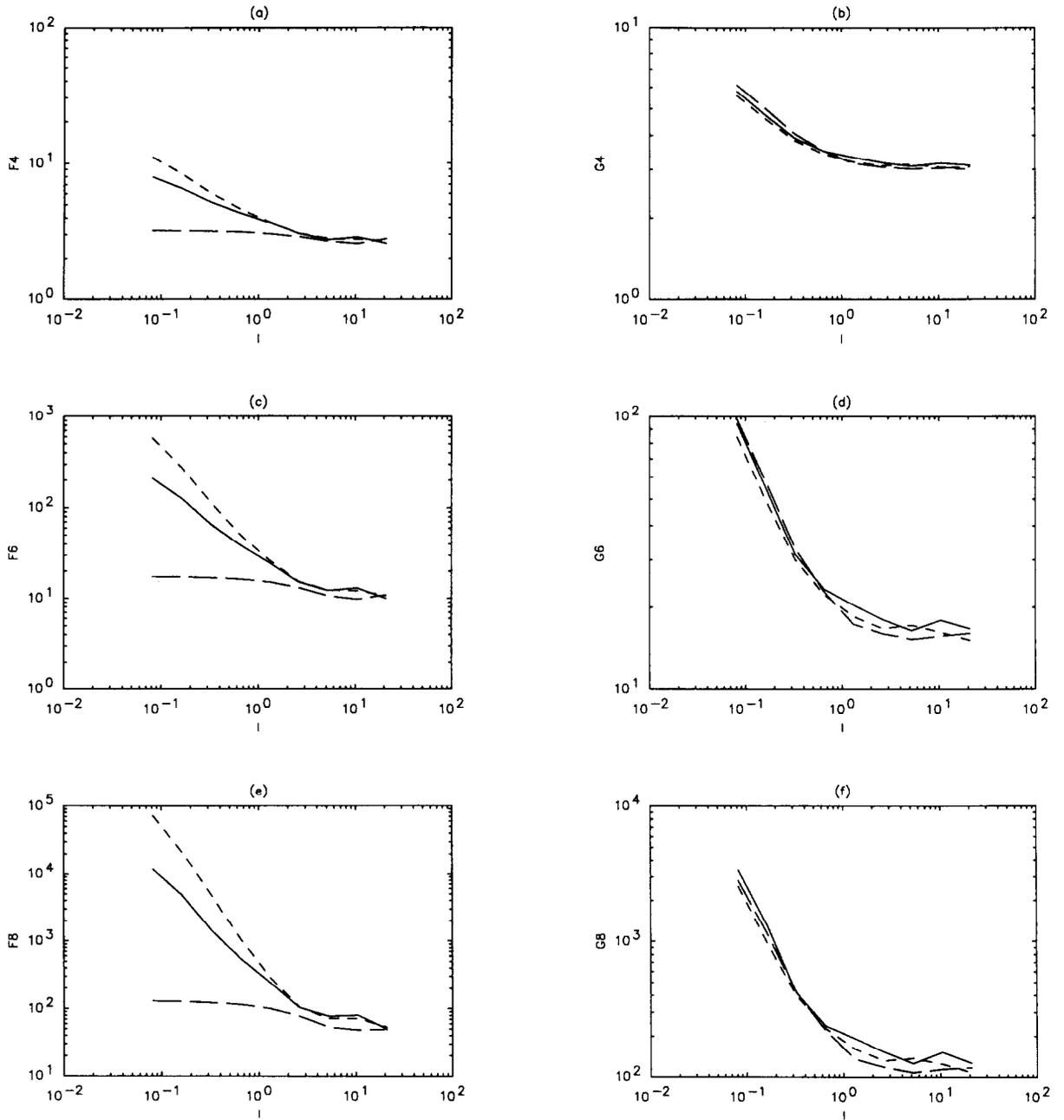
Fig. 3. F_l^{2j}, G_l^{2j}, $j=2, 3, 4$, for $L=6.7$ emphasizing the small-scale statistics $l < k_0^{-1}$. $\mathscr{C}=0.1$ (full lines), $\mathscr{C}=1$ (short dashes), $\mathscr{C}=5$ (long dashes). For Gaussian statistics, the normalized moments have the values 3, 15, 105 for $j=2, 3, 4$, respectively.

ticular of the density and the vorticity increments $\delta n_l = n(x+l) - n(x)$, $\delta \omega_l = \omega(x+l) - \omega(x)$, with $l = l\hat{x}$ or $l\hat{y}$,

$$F_l^{\{2j\}} = \frac{\langle (\delta n_l)^{2j} \rangle}{\langle (\delta n_l)^2 \rangle^j}, \quad G_l^{\{2j\}} = \frac{\langle (\delta \omega_l)^{2j} \rangle}{\langle (\delta \omega_l)^2 \rangle^j}. \quad (7)$$

The results are illustrated in Figs. 3, 4, where
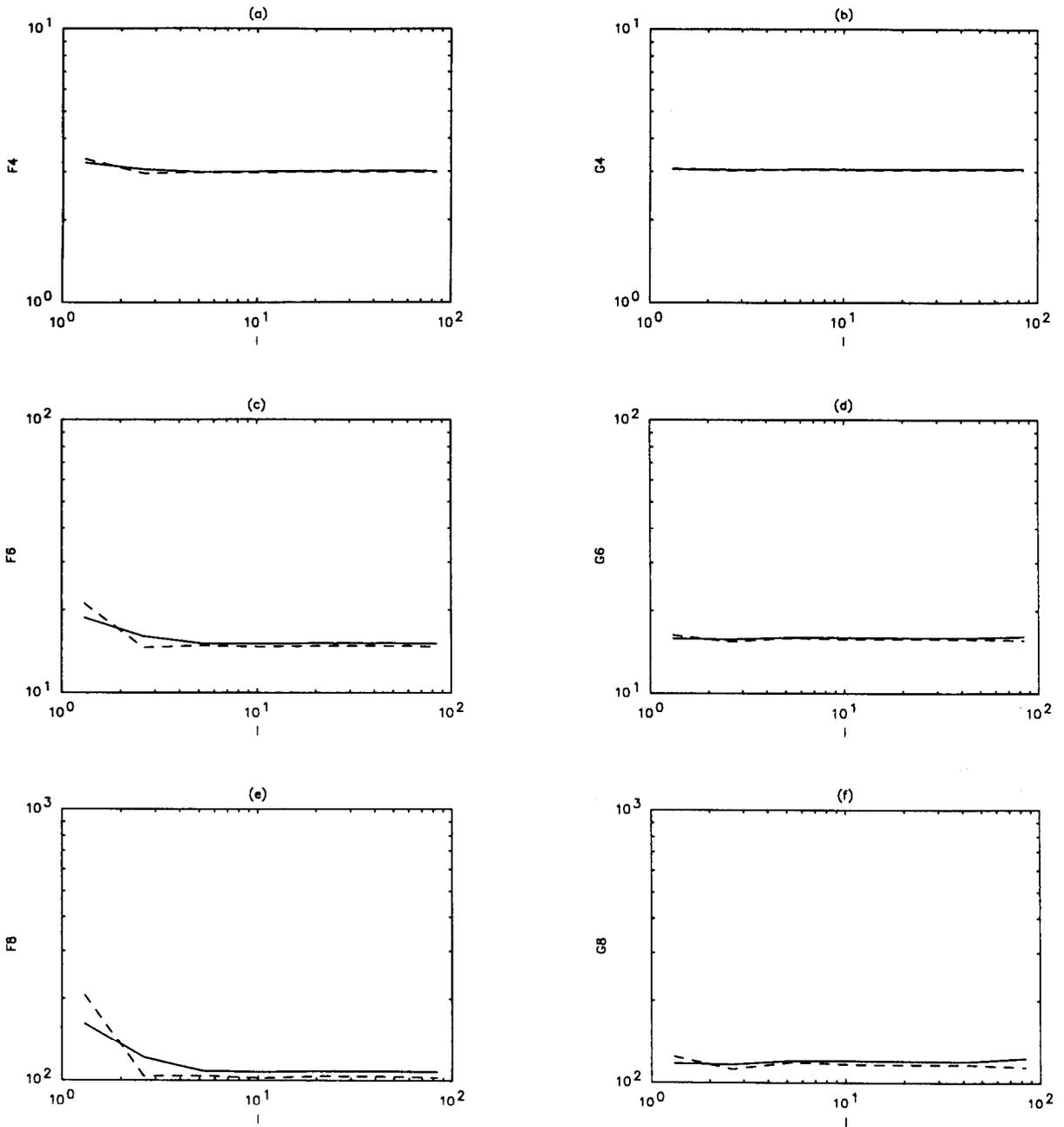
Fig. 4. F_l^{2j}, G_l^{2j}, $j = 2, 3, 4$, for large box size ($L = 26.7$) emphasizing the large-scale statistics $l > k_0^{-1}$, with increments in the x-direction. $\mathscr{C} = 0.1$ (full lines), $\mathscr{C} = 1$ (dashed lines). For Gaussian statistics, the normalized moments have the values 3, 15, 105 for $j = 2, 3, 4$, respectively.

$l_{min} = 2\pi L / (N/2)$ (N^2 is the number of grid-points) and $l_{max} = 2\pi L / 2$. Fig. 3 gives the structure functions for $L = 6.7$ and high spatial resolution (1024^2), em-

phasizing the small-scale statistics. Since the turbulence is isotropic at small scales, moments are averaged over both x and y directions. While the large-

scale statistics ($l \gtrsim k_0^{-1}$) are essentially Gaussian (it is in fact perfectly Gaussian as discussed below), we see that for $l < k_0^{-1}$ statistics become increasingly non-Gaussian indicating small-scale intermittency of the turbulence. In fact F_l^{2j} and G_l^{2j} show a clear power-law (or scaling) behavior, $F_l^{2j} \sim l^{\beta_j}$, $G_l^{2j} \sim l^{\gamma_j}$. Both β_j and γ_j are found to increase with j more strongly than linearly, which can be described in the framework of multifractality (well-known from hydrodynamic turbulence, see e.g. Ref. [12]). While γ_j is independent of $\mathscr{C}$ as is the kinetic energy spectrum (Fig. 1b), β_j varies with $\mathscr{C}$. We find $\beta_j \simeq \gamma_j$ for small $\mathscr{C}$, increasing slightly for $\mathscr{C} \to 1$, where $\beta_j \simeq 1.5\gamma_j$, and becoming very small $\beta_j \simeq 0$ for large $\mathscr{C}$, where $n_k \simeq \varphi_k$. The statistics of the potential increments $\delta\varphi_l$ are found to be Gaussian for all scales l independently of $\mathscr{C}$.

In order to determine if the large-scale statistics, $l \gtrsim k_0^{-1}$, were accurate, simulations with larger box size $L = 26.7$ with a grid-size 256^2 are followed over many large-eddy turnover times e.g. $t \simeq 50\tau_0$ for $\mathscr{C} = 5$, where $\tau_0 \simeq 10$, $\tau_0 = (uk_0)^{-1}$ and $u^2 = E^V/(2\pi)^2$. As seen in Fig. 4, the large-scale statistics are almost perfectly Gaussian. Only the case with $l = l\hat{x}$ is shown, but for $l = l\hat{y}$ results are virtually identical in spite of the anisotropy of the spectrum for $l \gtrsim k_0^{-1}$. The Gaussian statistics are consistent with the absence of conspicuous coherent structures, which is in contrast to the behavior found for more strongly viscous conditions [5]. A possible reason for this difference is the higher level of small-scale fluctuations in our case, which seems to destroy long-living structures. By considering dissipation terms of the form

$$\mathscr{D}^\omega = \nu_\omega \Delta^3 \omega, \quad \mathscr{D}^n = \nu_n \Delta n, \quad \nu_\omega = \nu_n = 0.01 , \quad (8)$$

we were able to reproduce the results of Ref. [5], obtaining long-living coherent structures and statistics far from Gaussian behavior. However, these coherent structures disappear for smaller dissipation coefficients and a higher order operator for the density

dissipation allowing an extended range of small-scale turbulence.

In summary, we have presented important features of resistive drift-wave turbulence, which serves as a paradigm of an autonomous (i.e. not externally driven) 2-D turbulence system with one inherent spatial scale k_0^{-1}, where k_0 is the position of the maximum of the energy spectrum, which depends on the adiabacity parameter $\mathscr{C}$. The turbulence is anisotropic at large scales $k < k_0$ reflecting the linear instability properties, but isotropic in the inertial range ($k > k_0$), where the spectra follow simple power laws. The statistics of the density and vorticity increments are non-Gaussian in the inertial range indicating increasing intermittency of small-scale fluctuations, but are perfectly Gaussian at the larger scales. The latter feature is consistent with the absence of isolated coherent structures, and is in contrast to the behavior of the simpler system of 2-D Navier–Stokes turbulence, which is dominated by large-scale self-organization.

References

[1] A. Hasegawa and M. Wakatani, Phys. Rev. Lett. 50 (1985) 682.
[2] M. Wakatani and A. Hasegawa, Phys. Fluids 27 (1984) 611.
[3] A. Hasegawa and K. Mima, Phys. Fluids 21 (1978) 87.
[4] B.D. Scott, H. Biglari, P.W. Terry and P.H. Diamond, Phys. Fluids B 3 (1991) 51.
[5] A.E. Koniges, J.A. Crotinger and P.H. Diamond, Phys. Fluids B 4 (1992) 2785.
[6] F.Y. Gang, B.D. Scott and P.H. Diamond, Phys. Fluids B 1 (1989) 1331.
[7] J.C. McWilliams, J. Fluid Mech. 146 (1984) 21.
[8] B. Legras, P. Santangelo and R. Benzi, Europhys. Lett. 5 (1988) 37.
[9] B.D. Scott, J. Comput. Phys. 78 (1988) 114.
[10] R.H. Kraichnan, J. Fluid Mech. 47 (1971) 525.
[11] R. Benzi, S. Patarnello and P. Santangelo, J. Phys. A 21 (1988) 1221.
[12] G. Paladin and A. Vulpiani, Phys. Rep. 156 (1987) 147.